

# Information on Polydispersity and Branching from Combined Quasi-Elastic and Integrated Scattering

W. Burchard,\* M. Schmidt, and W. H. Stockmayer†

*Institut für Makromolekulare Chemie der Albert-Ludwigs-Universität,  
D-7800 Freiburg i.Br., West Germany. Received December 26, 1979*

**ABSTRACT:** Several quantities sensitive to branching density and branching type and to molecular polydispersity can be obtained from quasi-elastic and integrated scattering measurements. These are the geometric and hydrodynamic branching factors ( $g = \langle S^2 \rangle_{z, \text{branched}} / \langle S^2 \rangle_{\text{linear}}$  and  $h = D_{\text{linear}} / D_{z, \text{branched}}$ ), the ratio  $\rho$  of geometric to hydrodynamic radii, the angular dependence of the particle scattering factor  $P_z(q)$ , and the first cumulant of the dynamic structure factor. Analytic expressions are given for these parameters for model regular and polydisperse star molecules, for branched polycondensates of the  $A_f$  and ABC types, and for randomly cross-linked chains. The utility of these parameters in distinguishing among different models is demonstrated with three examples.

## Introduction

Since the fundamental theory of branching and gelation was developed,<sup>1-3</sup> more than 30 years ago, a number of special models have been studied with regard to their molecular and structural properties, i.e., the molecular weights  $M_w$  and  $M_n$ , the mean-square radius of gyration  $\langle S^2 \rangle_z$ , the particle scattering factor  $P_z(q)$ , where  $q = (4\pi/\lambda) \sin(\theta/2)$ , and the intrinsic viscosity.<sup>4-26</sup> Fairly complicated structures are now accessible to calculation if kinetic data of sufficient accuracy are at hand. Quite often, however, and in particular with biological materials, these kinetic data are not available, and it is then especially important to consider what information on branched structure and molecular polydispersity can be extracted from measurements in dilute solutions. A few years ago, a brief review on the particle scattering factors of branched macromolecules was given by one of us,<sup>19</sup> and it was shown that indeed some information can be obtained from integrated scattering (IS) measurements. For this purpose, the molecules must have dimensions of the order of the wavelength of the scattering beam. This condition is often much easier to realize with branched materials than with linear chains, but it still represents a significant limitation in applicability. With the recent rapid development of equipment for dynamic "quasi-elastic" scattering (QES), smaller molecules have also become accessible to measurements of structural properties.<sup>27,28</sup> Parallel to this development in technology, recent calculations of QES for some branched models<sup>29-31</sup> have revealed a number of new features. It thus appears worthwhile to examine how these results, in combination with IS data, can be applied to the practical analysis of unknown structures. The present considerations are restricted to molecules in the unperturbed state, and refinements will be necessary in the future to allow for the effect of excluded volume. There is much evidence, however, that the effects of branching and the often vast polydispersity of the products are much more important than the influence of excluded volume,<sup>9,10,32-34</sup> and so the conclusions drawn in this study can be expected to remain valid to a considerable extent for good solvents.

The following data can be obtained from IS and QES experiments without reference to any special model. (a) Integrated scattering:  $M_w$ ,  $\langle S^2 \rangle_z$ , and  $P_z(q)$ ; (b) quasi-elastic scattering:  $D_z$ ,  $\lim_{q \rightarrow 0} d(\Gamma/q^2)/dq^2$ ,  $\Gamma/q^2 = f(q)$ , where  $D_z$  is the  $z$  average of the translational diffusion

constant and  $\Gamma = -[d \ln S(q, t)/dt]_{t=0}$  is the first cumulant of the dynamic structure factor  $S(q, t)$ . The diffusion constant  $D_z$  can be measured for small and large molecules, and the same is possible, in principle, for  $M_w$ , although some difficulties in integrated light scattering must be overcome for very low molecular weights. For reliable evaluation of the mean-square radius of gyration  $\langle S^2 \rangle_z$  and the initial slope of  $\Gamma$  as function of  $q^2$ , the molecules must be larger than about  $\lambda/10$ , and, in order to assess angular dependencies for  $P_z(q)$  and  $\Gamma/q^2$ , which deviate from linearity when plotted against  $q^2$ , the ratio  $\langle S^2 \rangle_z^{1/2}/\lambda$  has to be of the order of unity or larger. The data from IS and QES can be combined in various ways and, as we shall show, quite interesting information on molecular structure and on polydispersity can be obtained by such combinations.

In addition to the initial slope, the shape of the dynamic structure factor can also be observed at longer times. Interpretation of this curve in terms of the various correlation times is scarcely feasible at present, since the effects of branching, internal modes of motion and of polydispersity cannot be properly separated.

We confine consideration to the following models: (1) monodisperse and polydisperse linear chains;<sup>29,31</sup> (2) regular and polydisperse star macromolecules;<sup>30,31</sup> (3)  $f$ -functional random polycondensates of the  $A_f$  type;<sup>30,31</sup> (4) polycondensates of the ABC type with constraints on the reactivity of the three functional groups A, B, and C;<sup>30</sup> (5) randomly cross-linked chains.

By polydisperse linear chains we mean specifically polymers which follow the Schulz-Zimm length distribution. The polydispersity is characterized by the parameter  $m = (P_w/P_n - 1)^{-1}$ , where  $P_w$  and  $P_n$  are the weight- and number-average degrees of polymerization. The regular stars need no explanation; the polydisperse stars have all the same number  $f$  of rays per molecule and the ray-length distribution is characterized by the polydispersity parameter  $m = 1$ ; i.e.,  $P_w/P_n = 2$ , which is Flory's "most probable distribution". The  $f$ -functional random polycondensates are obtained from monomer units with  $f$  identical functional groups. In contrast to this type, the ABC polycondensates result from a monomer with three dissimilar functional groups A, B, and C, and the reaction is subject to the constraint that group B or group C can react with group A but all other reactions are excluded. Finally, in the model of randomly cross-linked chains the primary chains have a "most probable" length distribution. The same type of polymer is also obtained in the copolymerization of monovinyl with divinyl monomers. Comb molecules<sup>15-18</sup> will not be considered here, partly

\*Permanent address: Department of Chemistry, Dartmouth College, Hanover, N.H. 03755.

Table I

Dependence of the Mean-Square Radii of Gyration  $\langle S^2 \rangle_z$  and the Translational Diffusion Constants  $D_z$  on the Weight-Average Degree of Polymerization  $P_w$  and the Corresponding Exponents  $\nu_S$  and  $\nu_D$  in the Double-Logarithmic Plots of  $\langle S^2 \rangle_z$  and  $D_z$  vs.  $P_w$  for Some Selected Models ( $A' = k_B T / 6^{1/2} \pi^{3/2} \eta_0 b$ )

model	$\langle S^2 \rangle_z / b^2$	$\nu_S$	$D_z / A'$	$\nu_D$
linear chains				
monodisperse	$1/6 P_w$	1	$(8/3) P_w^{1/2}$	$-1/2$
polydisperse ( $m = 1$ )	$1/4 P_w$	1	$(2\pi/P_w)^{1/2}$	$-1/2$
polydisperse ( $m$ coupled chains)	$\frac{1}{6} \frac{m+2}{m+1} P_w^a$	1	$\left(\frac{\pi}{m+1}\right)^{1/2} 2 \sum_{k=1}^m \left(1 + \frac{k-1}{m}\right) c(k) / P_w^{1/2}$	$-1/2$
star molecules				
regular stars	$\frac{1}{6} \frac{3f-2}{f^2} P_w^b$	1	$\frac{8(2-f) + 2^{1/2}(f-1)}{3(fP_w)^{1/2}}$	$-1/2$
polydisperse stars	$\frac{f}{(f+1)^2} P_w$	1	$\left(\frac{\pi}{f+1}\right)^{1/2} \frac{f+3}{2P_w^{1/2}}$	$-1/2$
polycondensates				
$A_f$ type	$\frac{f-1}{2f} P_w^c$	1	$\left(\frac{\pi f}{(f-1)P_w}\right)^{1/2}$	$-1/2$
ABC type	$\frac{1+2B}{4(1+B)^2} P_w^d$	$1/2$ to 1	$\pi^{1/2} \frac{2+B}{[2(1+B)P_w]^{1/2}}$	$-1/4$ to $-1/2$
randomly cross-linked chains (polydisperse ( $m = 1$ ) primary chains)	$\frac{P_w^e}{2(2+\epsilon^*)}$	1	$\pi^{1/2} \left(\frac{2(1+\epsilon^*)^{1/2}}{P_w}\right)$	$-1/2$

<sup>a</sup>  $m$  = polydispersity parameter;  $m^{-1} = P_w/P_n - 1$ , where the subscripts denote weight- and number-average degrees of polymerization.<sup>30</sup> <sup>b</sup>  $f$  = number of rays per star (functionality of the star center). <sup>c</sup>  $f$  = functionality of the monomeric unit. <sup>d</sup>  $B = p(1-p)/(1-\alpha)$ , where  $p$  is the branching probability and the link probability  $[(1-\alpha)^{-1} = P_n]$ .  $B$  is very nearly the number of branching points per molecule based on the number-average degree of polymerization  $P_n$ . <sup>e</sup>  $\epsilon^* = \epsilon(n-1)x$ , where  $\epsilon$  is the probability that a pendant double bond has been involved in a cross-link.  $n-1$  is the number of pendant vinyl double bonds per multifunctional vinyl monomer, and  $x$  is the molar fraction of multifunctional vinyl monomers in the branched molecule.

because of the unsettled question as to whether the number of grafted chains and their length appreciably affect the flexibility of the backbone.

### Molecular Weight Dependence of $\langle S^2 \rangle_z$ and $D_z$ . The Ratios $g$ and $h$

To avoid misunderstanding, we stress that we are dealing here always with *unfractionated* samples. Considerations are therefore based on those molecular averages which are *directly measurable* by the two scattering techniques.

Quite often the conditions of polymerization can be varied systematically so that samples of different molecular weight can be synthesized. A reasonable and widely used first method of characterization is to plot global structural properties, e.g., the mean-square radius of gyration  $\langle S^2 \rangle_z$  or the translational diffusion constant  $D_z$ , against the molecular weight  $M_w$ . Such plots alone, however, give little information, since usually straight lines are obtained on double-logarithmic plots with slopes which in the former case are often somewhat larger than unity (because of excluded-volume effects). In rare cases the exponents are smaller than unity; then, however, one has clear evidence for branching, as will be shown below. If the measurements are carried out under  $\Theta$  conditions, the exponents given in Table I will be observed.

More instructive than the molecular weight dependence is a comparison with the corresponding properties of well-characterized reference samples. In many cases, the molecular weight relationships of well-fractionated or monodisperse linear chains are known, and such monodisperse chains are therefore usually taken for reference. Other choices would be possible and perhaps even more sensible: for instance, to characterize  $f$ -functional random polycondensates, it would be probably more useful to take *unfractionated* linear bifunctional random polyconden-

sates for reference. In standard practice two characteristic factors are defined: for the geometric dimensions<sup>4</sup>

$$g = \langle S^2 \rangle_z / \langle S^2 \rangle_{l, \text{mono}} \quad (\text{both at the same } P_w) \quad (1)$$

and for the hydrodynamic dimensions<sup>12</sup>

$$h = D_{l, \text{mono}} / D_z \quad (\text{both at the same } P_w) \quad (2)$$

where the subscript  $l, \text{mono}$  denotes a linear monodisperse reference material. These two definitions deviate slightly but significantly from the original definitions by the fact that the observable radii are compared here at same *weight-average* degree of polymerization, while Zimm and Stockmayer introduced for polydisperse samples the so-called  $g_z$  factor, where the radii are compared at same *z-average* degree of polymerization. Since in this study we wish to use only quantities which are actually directly measured by IS or QES, we prefer the above definitions; indeed, the *z-average* molecular weight is not unambiguously measurable by means of light scattering. It is necessary to emphasize that in spite of this apparently minor change in definition the resulting differences in  $g$  and  $h$  can be substantial because of the huge polydispersity observed quite frequently with randomly branched samples. Table II gives  $g$  and  $h$  for the models of Table I.<sup>35,36</sup>

The quantities  $g$  and  $h$ , so defined, have some surprising features. It is commonly presumed that  $g$  and  $h$  are continuously decreasing functions of the branching density and always smaller than unity. This statement is certainly correct for monodisperse samples and also holds for regular stars. In the other cases, however,  $g$  and  $h$  are larger than unity for low branching densities, and in the case of randomly branched polycondensates or randomly cross-linked molecules they even *increase* with the number of functional groups, in contrast to the decrease for star molecules (see Figures 1 and 2). The reason for this behavior is that

Table II  
Geometric and Hydrodynamic Factors for Some Selected Models

model	$g$	$h$
linear chains		
monodisperse	1	1
polydisperse ( $m = 1$ )	$3/2$	$\frac{4}{3} \left( \frac{2}{\pi} \right)^{1/2}$
polydisperse ( $m$ coupled chains)	$\frac{m+2}{m+1}$	$\frac{4}{3} \left( \frac{m+1}{\pi} \right)^{1/2} \left/ \left( \sum_{k=1}^m \left( 1 - \frac{k-1}{m} \right) c(k) \right)^a \right.$
star molecules		
regular stars	$\frac{3f-2}{f^2}$	$\frac{f^{1/2}}{(2-f) + 2^{1/2}(f-1)}$
polydisperse stars	$\frac{6f}{(f+1)^2}$	$\frac{16}{3(f+3)} \left( \frac{f+1}{\pi} \right)^{1/2}$
polycondensates		
$A_f$ type	$\frac{3(f-1)}{f}$	$\frac{8}{3} \left( \frac{f-1}{\pi f} \right)^{1/2}$
ABC type	$\frac{3}{2} \frac{1+2B}{(1+B)^2}$	$\frac{8}{3} \frac{[2(1+B)]^{1/2}}{\pi^{1/2}(2+B)}$
randomly cross-linked chains (polydisperse ( $m = 1$ ) primary chains)	$\frac{3}{2(1+\epsilon^*/2)}$	$\frac{8}{3} \left( \frac{1}{2\pi(1+\epsilon^*)} \right)^{1/2}$

<sup>a</sup> For the definition of  $c(k)$  see ref 30.

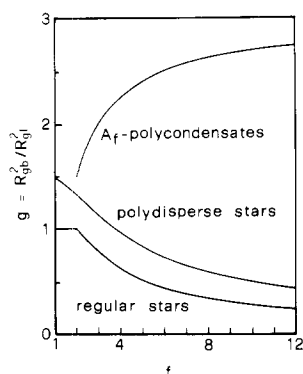


**Figure 1.** Dependence of the geometric branching factor  $g$  on the number of functional groups  $f$  for three models.  $f$  denotes the number of rays per star molecule and, in the case of the polycondensates, the number of functional groups per monomeric unit,  $R_g = \langle S^2 \rangle_z^{1/2}$  is the radius of gyration, and the subscripts b and l denote branched and linear molecules.

polydispersity causes a larger increase of the  $z$ -average mean-square radius of gyration than the corresponding increase of the weight-average molecular weight. Thus  $g$  and  $h$  embody two effects with converse behavior: polydispersity, which causes an increase, and branching, which causes the familiar decrease. For the randomly branched chains the extraordinarily broad molecular distribution dominates the high branching density of the individual molecules. The decrease of the two characteristic factors  $g$  and  $h$  with increasing number of rays for the polydisperse stars is to a large extent also a consequence of a narrowing of the molecular weight distributions.

The lack of one-to-one correspondence between  $g$  and  $h$  and the branching density may be regretted, but on reflection the inverse behavior of the randomly branched and the starlike-branched polymers proves to be advantageous because a combination of  $g > 2$  and  $h > 1$  is a clear indication for a random-branching process with its very broad molecular weight distribution, while values below unity indicate less pronounced polydispersities. Sometimes  $g$  and  $h$  decrease with increasing molecular weight. Such

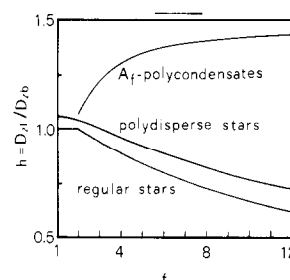


**Figure 2.** Dependence of the hydrodynamic branching factor  $h = D_z/D_{zb} = \langle R_{hl}^{-1} \rangle / \langle R_{hb}^{-1} \rangle_z$  on the number of functional groups  $f$  for three models.  $R_h$  is the hydrodynamic radius defined by eq 3; all other notation is as in Figure 1.

behavior is observed, for instance, with the ABC-type polycondensates, and in these cases the exponents  $\nu_s$  and  $\nu_D$  in the molecular weight dependencies of  $\langle S^2 \rangle_z$  and  $D_z$  become less than 1 or  $1/2$ , respectively. Here the increase of branch points is no longer overshadowed by the increase in polydispersity, which is much less pronounced than for the random  $A_f$ -type polycondensates.<sup>19</sup>

### The $\rho$ Ratio

Another quantity of interest arises from the combination of  $\langle S^2 \rangle_z$  and  $D_z$ . First we define an effective  $z$ -average Stokes–Einstein hydrodynamic radius by

$$D_z = \frac{k_B T}{6\pi\eta_0} \left\langle \frac{1}{R_h} \right\rangle_z \quad (3)$$

We can now define a dimensionless quantity

$$\rho = \langle R_h^{-1} \rangle_z \langle S^2 \rangle_z^{1/2} \quad (4)$$

which no longer depends on the bond length and the degree of polymerization but is a function of the branching density, of polydispersity, and of the inherent flexibility of the subchains. A factor similar to eq 4 was used years ago to demonstrate the transition of a wormlike chain from rodlike to random-coil behavior.<sup>37</sup> There, however, the end-to-end distance was used, which is not directly

Table III  
 $\rho$  Factor and Molecular Polydispersity  $P_w/P_n$  for Some Selected Models<sup>a</sup>

model	$\rho$	$P_w/P_n$
linear chains		
monodisperse	$8/3\pi^{1/2}$	1
polydisperse ( $m = 1$ )	$3^{1/2}$	2
polydisperse ( $m$ coupled chains)	$\frac{(m+2)^{1/2}}{m+1} 2\sum \left(1 + \frac{k-1}{m}\right) c(k)$	$1 + (1/m)$
star molecules		
regular stars	$\left(\frac{3f-2}{f\pi}\right)^{1/2} \frac{8(2-f) + 2^{1/2}(f-1)}{3f}$	1
polydisperse stars	$\left(\frac{6f}{f+1}\right)^{1/2} \frac{f+3}{2(f+1)}$	$1 + (1/f)$
polycondensates		
A <sub>f</sub> type	$3^{1/2}$	$P_w \left(1 - \frac{f}{2(f-1)}\right)$
ABC type	$\left(\frac{3}{4} \frac{1+2B}{1+B}\right)^{1/2} \left(\frac{2+B}{1+B}\right)$	$2(1+B)$
randomly cross-linked chains (polydisperse ( $m = 1$ ) primary chains)	$3^{1/2}$	$2(P_w/P_n p)$
monodisperse spheres	$(3/5)^{1/2}$	1

<sup>a</sup>  $\rho = \langle 1/R \rangle_z \langle S^2 \rangle_z^{1/2}$ ; all other notation is as in Tables I and II.

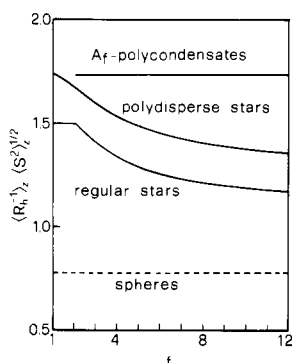


Figure 3. Dimensionless parameter  $\rho = \langle R_h^{-1} \rangle_z R_g$  for three branching models and for compact spheres.

measurable. Table III gives a list of the  $\rho$  factors for the models of Tables I and II and also for compact spheres (see also Figure 3).

#### Initial Slope of $\Gamma/q^2 D_z$ as a Function of $u^2 = q^2 \langle S^2 \rangle_z$

The initial slope of the particle scattering factor from IS, when plotted against  $u^2 = q^2 \langle S^2 \rangle_z$ , is always  $1/3$  for any model. In contrast, the quantity  $q^2 \Gamma$ , when plotted against  $u^2$ , has an initial slope that is significantly structure dependent<sup>31</sup> and can be used as additional information if the polymers are large enough. Table IV gives values of this slope for the various models (see also Figure 4).

#### Interdependence of the First Cumulant and the Particle Scattering Factor

For large objects, where  $\langle S^2 \rangle_z^{1/2}/\lambda > 1$ , the first cumulant and the particle scattering factor exhibit characteristic deviations from linear behavior. One can use such data in three ways: (i) to study the particle scattering factor  $P(q)$  at larger  $u^2$ , (ii) to study  $\Gamma/q^2 D_z$  at larger angles, and (iii) to study the interdependence of  $\Gamma$  and  $P(q)$ .

Method i was discussed in some detail in a previous paper,<sup>19</sup> where it was pointed out that instructive conclusions can be drawn in particular from the so-called Kratky plot, i.e., a plot of  $u^2 P(q)$  against  $u^2$ . The appearance of a maximum, its position, and its height are characteristic for special branching types and polydispersity.

The second method, i.e., a plot of  $\Gamma/q^2 D_z$  against  $u^2$ , requires measurements of high accuracy. There are some

Table IV  
Particle Scattering Factor  $P_z(q)$ , First Cumulant  $\Gamma(q)$ , and the Coefficient  $C$  in the Initial Slope of  $\Gamma = D_z q^2 (1 + Cu^2 - \dots)$  for A<sub>f</sub> and ABC Polycondensates and for Cross-Linked Chains<sup>a</sup>

A<sub>f</sub>-Random Polycondensates and Randomly Cross-Linked Polydisperse Chains

$$P_z(q) = (1 + u^2/3)^{-1}$$

$$\Gamma = q^2 D_z (1 + u^2/3) \left[ 1 + \frac{u^2(1 + u^2/3)^{1/2}}{30(1 + a^2 u^2/3)^{3/2}} \right]$$

$$C = 1/5$$

ABC Polycondensates

$$P_z(q) = \frac{(1 + v^2)^{-1} + B(1 + v^2)^{-2}}{1 + B}$$

$$\Gamma = \Gamma_{\text{pre}} + \Delta \Gamma$$

$$\Gamma_{\text{pre}} = q^2 D_z (1 + v^2)^{1/2} \frac{1 + v^2/(1 + B/2)}{1 + v^2/(1 + B)}$$

$$\Delta \Gamma = \Gamma_{\text{pre}} \frac{v^2}{10} \frac{(1 + v^2)^{3/2}}{(1 + a^2 v^2)^{5/2}} \frac{(1 + a^2 v^2) + 3/2 B}{(1 + v^2) + B/2}$$

$$C = \frac{1}{6} \frac{1 + B}{1 + 2B} \left( 1 + \frac{1}{5} \frac{2 + 3B}{2 + B} + \frac{B}{(1 + 2B)(2 + B)} \right)$$

where

$$B = \frac{p(1-p)}{1+B} \frac{P_w}{2}$$

and

$$v^2 = \frac{1}{3} \frac{1 + B}{1 + 2B} u^2$$

<sup>a</sup> For derivation see Appendix. The corresponding relationships for linear and star-branched molecules are given in ref 31.

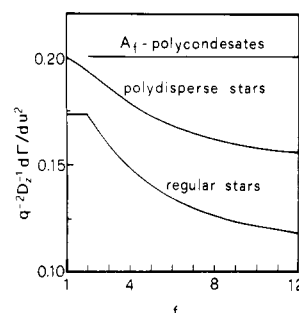
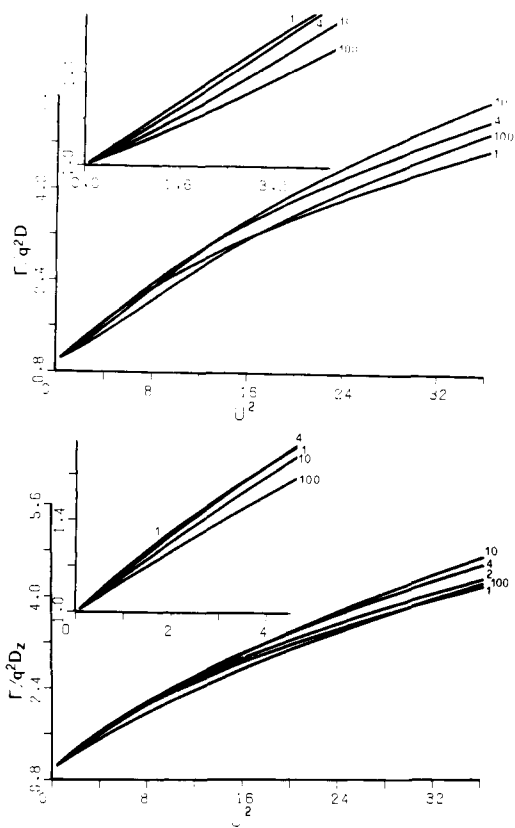
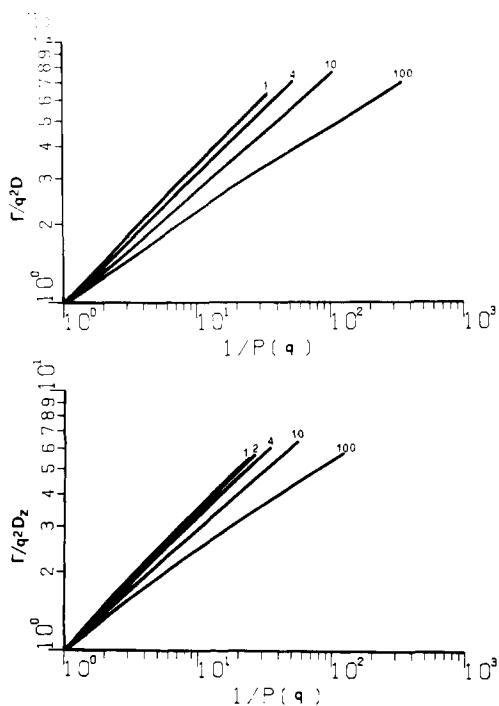


Figure 4. Coefficient  $C$  in the initial slope of  $\Gamma = q^2 D_z (1 + Cu^2 - \dots)$  for three branching models.



**Figure 5.** Angular dependence of the first cumulant  $\Gamma$  in a plot of  $\Gamma/q^2 D_z$  against  $u^2 = \langle S^2 \rangle_z q^2$  for monodisperse (top) and for polydisperse (bottom) star molecules. The numbers on the curves denote the number of rays per molecule. Inserts show behavior at small  $u^2$ . Note the slight upturn at  $u^2 \approx 2$  for monodisperse stars with more than 4 rays which is missing for polydisperse stars. The function  $\Gamma/q^2 D_z$  is normalized to 1 at  $q^2 = 0$ .



**Figure 6.** Interdependence of the normalized first cumulant and the reciprocal particle scattering factor for monodisperse (top) and for polydisperse (bottom) star molecules.

differences in behavior for the various models. For instance, regular stars show a weakly pronounced sigmoidal curve with a slight upturn at intermediate  $u^2$  before the

curve bends down. This upturn is missing for polydisperse stars (see Figure 5).

The third method, namely, a plot of  $\Gamma/q^2 D_z$  against  $1/P_z(q)$  on a double-logarithmic scale, probably gives the most instructive insight. (Figure 6 gives examples for regular and polydisperse stars. These curves include monodisperse and polydisperse linear chains ( $f = 1$ ) and  $f$ -functional random polycondensates.) This may be recognized from Table IV, where the particle scattering factors and the first cumulants of the various models are collected. The reason for the striking coincidence of the scattering behavior between linear polydisperse chains (with the "most probable distribution") and  $f$ -functional polycondensates has been discussed previously<sup>9,19</sup> and arises from the fact that the length distribution of subchains (i.e., the number of subchains of a given length in the polymer) is identical and follows a "most probable distribution" in these polymers. This statement does not hold for monodisperse chains or for star molecules and ABC-type polycondensates. For values of  $1/P_z(q) < 10^2$  the double-logarithmic plot of the first cumulant against the reciprocal particle scattering factor yields a straight line to a good approximation. In this case the exponent  $\nu$  is related to the initial slope  $C$  of  $\Gamma/q^2 D_z$  against  $u^2$  by the equation

$$\Gamma/q^2 D_z = [P_z(q)]^{-\nu} \quad (5)$$

with

$$\nu = 3C \quad (5a)$$

which immediately follows from the power expansion

$$1 + Cu^2 = (1 + \frac{1}{3}u^2)^\nu = 1 + (\nu/3)u^2 + \dots$$

## Discussion

The utility of the various quantities given in the four tables may be elucidated by a few examples.

(i) Let us assume that the following parameters have been measured under  $\Theta$  conditions:  $g = 0.77$ ,  $h = 0.94$ ,  $\rho = 1.4$ , and  $C = 0.158$ . We immediately see from Figures 1–4 that none of these parameters fits a randomly branched polymer. The question remains whether the measured set of parameters will suffice for distinguishing between the models of star polymers and the ABC-type polycondensate. First, it will be noticed that the formulas for the polydisperse stars and the ABC polycondensates give formally identical results when  $B$  is replaced by  $(f-1)/2$ , with the decisive difference that  $f$  in the star molecules is a constant number while  $B$ , the number of branching points in the ABC polycondensate, increases as the polymer becomes larger. From Figures 1–4 we read off

	$f$		$B$
	reg stars	polydisp stars	ABC polycondensate
$g = 0.77 \pm 14\%$	$3 \pm 0.8$	$5.5 \pm 1.4$	$2.25 \pm 0.6$
$h = 0.94 \pm 5\%$	$3 \pm 0.8$	$4.3 \pm 0.9$	$1.65 \pm 0.35$
$\rho = 1.4 \pm 6\%$	$3 \pm 0.9$	$8.0 \pm 2.5$	$3.5 \pm 1.1$
$C = 0.158 \pm 10\%$	$3 \pm 1.5$	$10.0 \pm 5$	$4.5 \pm 2.3$

This situation would give clear evidence for a regular star with three arms. The measurements are, of course, charged with certain errors. The mean-square radius of gyration can be measured with an accuracy of  $\pm 10\%$  and the diffusion constants with an accuracy of better than  $\pm 3\%$ , which would yield the percentage errors indicated above. It thus turns out that of the four listed quantities the  $\rho$  parameter is the most reliable and sensitive to structural differences. Still, at least two of the four quantities have

to be measured before a distinction between the various models becomes possible, and the next best quantity after  $\rho$  is  $h$  because of the high accuracy of measurements of  $D_z$  from QELS. In order to distinguish between polydisperse stars and a polymer of the ABC type, one must perform measurements at different molecular weights, where the different species could, in this case, be obtained also by fractionation. If star molecules are present, the factors should shift to those for monodisperse regular stars, while those for the ABC polycondensates would show a pronounced molecular weight dependence.

(ii) For poly(vinyl acetates) prepared by emulsion polymerization a value of  $\rho = 1.84$  is found<sup>38</sup> at low monomer conversion, and thus gradually decreases to  $\rho = 1.70$  at  $M_w = 10.6 \times 10^6$ . At higher extents of reaction, when a molecular weight about  $M_w = 15 \times 10^6$  is reached, the parameter  $\rho$  shows a steep decrease to 0.55. A geometric  $g$  factor or a hydrodynamic  $h$  factor could not be measured since no calibration curve for linear PVAc in methanol was available. The coefficient  $C$  from the initial slope of the first cumulant was found to scatter around a value of 0.2.

The high value of  $\rho$  at low conversions is only slightly greater than the ideal figure of  $3^{1/2}$  for polydisperse linear or randomly branched systems, and this is not unexpected as long as the individual polymer molecules are appreciably smaller than the latex particle containing them. In this region, the angular dependence of the integrated light scattering also shows behavior typical of randomly branched macromolecules. The slight decrease of  $\rho$  with increasing molecular weight is, on the other hand, an indication that the branching process is not fully random. This deviation from randomness may have its origin in the restricted space available to the polymer, but it also may be based on the chain-transfer mechanism which shows some similarities to ABC-type polycondensation.<sup>21</sup>

The observed<sup>38</sup> steep decrease of the  $\rho$  factor around  $M_w = 15 \times 10^6$  has its roots in the fact that the branched molecules have reached the dimensions of the latex particle such that at least one big macromolecule expands over the whole volume. At still higher conversion, this gelled macromolecule more and more completely fills the latex volume, thereby preserving the spherical shape of the latex particle, even when the external boundary of the soap is removed. The  $\rho$  factor is now much smaller than for any branching model discussed here, and the value is close to that of a compact sphere. This conclusion is supported by the angular dependence of the integrated light scattering which also gives evidence for the spherical shape of the gelled particles.<sup>39,40</sup>

(iii) The third example refers to a  $\beta$ -limiting dextrin of amylopectin measured by ILS and QELS in aqueous 1 N NaOH. This limiting dextrin was obtained from amylopectin by the action of  $\beta$ -amylase, which degrades the outer chains of the branched polymer. The  $g$  and  $h$  factors could not be measured in this case, since the amylopectin has a molecular weight ( $\pm 15\%$ )  $M_w = 500 \times 10^6$ <sup>41,42</sup> and linear amylose samples of such high molecular weight are not available. Both ILS and QELS exhibit strong angular dependence, and the double-logarithmic plot of  $\Gamma/q^2 D_z$  against  $P_z(q)^{-1}$  gives a straight line with an exponent of  $\nu = 0.39$ . Measurements<sup>42</sup> of the radius of gyration,  $\langle S^2 \rangle_z^{1/2} = 490$  nm, and of the diffusion coefficient,  $D_z = 7.1 \times 10^{-13}$  m<sup>2</sup> s<sup>-1</sup>, lead to  $\rho = 0.89$ .

For a long time amylopectin was believed to be representative of the ABC-type polycondensate.<sup>43,44</sup> For this model we find in the limit of a large number of branching points the asymptotic exponent  $\nu = 0.40$ , which is close to the experimentally observed value. This result can be

cross-checked, since the branching density can be determined chemically and has long been known to be  $p = 0.04$ . The number of branching points  $B$  is related to an ABC-type polycondensate to the branching density  $p$  and the weight-average degree of polymerization  $P_w$  by the equation (see Appendix)

$$p(1-p)P_w = 2B(1+B) \quad (6)$$

from which we find  $B = 250$ ; this leads to (Table IV)  $\nu = 0.401$ , which in fact is the asymptotic value.

While the above exponent is in good agreement with the ABC-type polycondensate, we find significant deviations from this model for the  $\rho$  factor and the particle scattering factor. According to the model,  $\rho$  can never decrease below 1.22, whereas a value of 0.89 is found experimentally. Also, the particle scattering factor should show a pronounced maximum at  $u^2 = 6$  in a Kratky plot, but this is not observed.<sup>19,41,42</sup> These two deviations reveal that the ABC-polycondensate cannot be a correct model for amylopectin. Similar conclusions have been drawn from degradation experiments with various specific enzymes.<sup>45</sup> The good agreement of the exponent  $\nu$  with the asymptote of the ABC model cannot be considered highly specific, since a similar asymptote may result for various other models. This last example shows that scattering experiments alone rarely, if ever, allow a unique determination of structure. With additional data from chemical or kinetic experiments, however, the rather simplified models discussed here can sometimes be realistically refined.

**Acknowledgment.** W.H.S. thanks the Alexander von Humboldt Stiftung for a Senior U.S. Scientist Award (1978–1979). W.B. and M.S. are grateful to the Deutsche Forschungsgemeinschaft for financial support.

#### Appendix. Derivation of Equations for $P_z(q)$ and $\Gamma$ Given in Table IV

All equations are easily obtained from the derivative of a general path weight generating function  $U_0(\phi_j)$ , where  $\phi_j$  is a special weighting function for a pair of elements joined by a chain of  $j$  monomeric units in length. The degree of polymerization  $P_w$ , the particle scattering factor  $P_z(q)$ , and the first cumulant of the time correlation function of the quasi-elastically scattered light  $\Gamma$  are obtained as

$$P_z(q) = P_w^{-1} U_0'(\phi_j = e^{-y^2 j}) \quad (A1)$$

$$P_w = U_0'(\phi_j = 1) \quad (A2)$$

$$\Gamma = [P_w P_z(q)]^{-1} [U_0'(\phi_j^{\text{QES}}) + q^2 k_B T / \zeta] \quad (A3)$$

where<sup>31</sup>

$$\phi_j^{\text{QES}} = q^2 A' \left[ j^{-1/2} e^{-y^2 j} + \frac{y^2}{5} j^{1/2} e^{-a^2 y^2 j} \right] \quad (A4)$$

and

$$\begin{aligned} y^2 &= b^2 q^2 / 6 \\ a^2 &= 0.72 \\ A' &= k_B T / 6^{1/2} \pi^{3/2} \eta_0 b \end{aligned} \quad (A5)$$

The path weight generating functions of the randomly cross-linked chains and the  $A_f$  and ABC type polycondensates were derived previously and are given below without derivation.<sup>9,19,46</sup>

**Randomly Cross-Linked Chains.** The derivative of the path weight generating function reads<sup>46</sup>

$$U_0'(\phi_j) = \phi_0 + 2\alpha[1 + \epsilon^*] \sum_{j=1}^{\infty} [\alpha(1 + \epsilon^*)]^{j-1} \phi_j \quad (\text{A6})$$

Here  $\alpha$  is the link probability for the formation of a primary chain and  $\epsilon^* = \epsilon(n-1)x$  is the cross-linking probability, where  $\epsilon$  is the probability that a pendant vinyl double bond has reacted and  $x$  is the mole fraction of the multifunctional vinyl comonomer with  $n$  vinyl double bonds per monomer. We assume long chains, where  $\alpha \simeq 1$ . Under such conditions  $\epsilon^*$  can be shown to be a small quantity. Hence

$$\alpha(1 + \epsilon^*) \simeq e^{-[1-\alpha(1+\epsilon^*)]} \quad (\text{A7})$$

Passing to integrals and neglecting terms of the order of unity, we find

$$P_w = 2\alpha(1 + \epsilon^*) \int_0^{\infty} e^{-[1-\alpha(1+\epsilon^*)]j} dj = \frac{2\alpha(1 + \epsilon^*)}{1 - \alpha(1 + \epsilon^*)} \quad (\text{A8})$$

$$P_z(q) = \frac{2\alpha(1 + \epsilon^*)}{P_w} \int_0^{\infty} e^{-[1-\alpha(1+\epsilon^*)+y^2]j} dj = \left[ 1 + \frac{y^2}{1 - \alpha(1 + \epsilon^*)} \right]^{-1} \quad (\text{A9})$$

and since  $P_z(q) = 1 - u^2/3 + \dots$ , we find by power expansion of eq A9

$$y^2/[1 - \alpha(1 + \epsilon^*)] = \frac{1}{3}u^2 \quad (\text{A10})$$

and finally

$$P_z(q) = (1 + u^2/3)^{-1} \quad (\text{A11})$$

Next (neglecting the free-draining term) we have

$$\Gamma = q^2 A' \left[ \int_0^{\infty} (j^{-1/2} e^{-[1-\alpha(1+\epsilon^*)+y^2]j} + (y^2/5)j^{1/2} e^{-[1-\alpha(1+\epsilon^*)+a^2y^2]j}) dj \right] / \int_0^{\infty} e^{-[1-\alpha(1+\epsilon^*)+y^2]j} dj \quad (\text{A12})$$

Integration yields

$$\Gamma = q^2 A' \pi^{1/2} \left\{ [1 - \alpha(1 + \epsilon^*)]^{1/2} \left[ 1 + \frac{y^2}{1 - \alpha(1 + \epsilon^*)} \right]^{1/2} \times \left( 1 + \frac{y^2}{10} \frac{(1 - \alpha(1 + \epsilon^*) + y^2)^{1/2}}{(1 - \alpha(1 + \epsilon^*) + a^2 y^2)^{3/2}} \right) \right\} \quad (\text{A13})$$

For  $q^2 \rightarrow 0$  one has  $\Gamma \rightarrow q^2 D_z$ ; thus

$$\Gamma = q^2 D_z (1 + u^2/3)^{1/2} \left[ 1 + \frac{u^2}{30} \frac{(1 + u^2/3)^{1/2}}{(1 + a^2 u^2/3)^{3/2}} \right] \quad (\text{A14})$$

where use was made of eq A9.

**A<sub>r</sub>-Type Polycondensates.** The same equations as for randomly cross-linked chains are obtained for A<sub>r</sub>-type polycondensates with<sup>9</sup>

$$U_0'(\phi_j) = \phi_0 + \alpha f \sum_{j=1}^{\infty} [\alpha(f-1)]^{j-1} \phi_j \quad (\text{A15})$$

**ABC-Type Polycondensates.** Here the derivative of the path weight generating function is<sup>19</sup>

$$U_0'(\phi_j) = \phi_0 + 2\alpha \sum_{j=1}^{\infty} \alpha^{j-1} \phi_j + 2\alpha(1-p)p \sum_{j=1}^{\infty} \alpha^{j-1} \sum_{k=1}^{\infty} \alpha^{k-1} \phi_{j+k} \quad (\text{A16})$$

Again  $\alpha \simeq 1 \simeq e^{-(1-\alpha)}$  and one easily finds

$$P_w = \frac{2}{1-\alpha} + \frac{2p(1-p)}{(1-\alpha)^2} = \frac{2}{1-\alpha}(1+B) \quad (\text{A17})$$

$$P_z(q) = \frac{(1+v^2)^{-1} + B(1+v^2)^{-2}}{1+B} \quad (\text{A18})$$

with

$$v^2 = \frac{y^2}{1-\alpha} = \frac{u^2}{3} \frac{1+B}{1+2B} \quad (\text{A19})$$

where the connection to  $u^2 = \langle S^2 \rangle_z q^2$  follows from the series expansion of  $P_z(q)$

$$\Gamma = 2 \left[ \int_0^{\infty} e^{-(1-\alpha)j} \phi_j^{\text{QES}} dj + p(1-p) \int_0^{\infty} \int_0^{\infty} e^{-(1-\alpha)(j+k)} \phi_{j+k}^{\text{QES}} dj dk \right] / P_w P_z(q) \quad (\text{A20})^{29}$$

Integration is conveniently performed by splitting  $\phi_j^{\text{QES}}$  into  $\phi_{j,\text{pre}} + \Delta\phi_j$ , whence one finds  $\Gamma = \Gamma_{\text{pre}} + \Delta\Gamma$ , with

$$\Gamma_{\text{pre}} = q^2 A' \pi^{1/2} (1-\alpha)^{1/2} (1+v^2)^{1/2} \frac{1+v^2+B/2}{1+v^2+B} \quad (\text{A21})$$

$$\Delta\Gamma = \Gamma_{\text{pre}} \frac{v^2}{10} \frac{(1+v^2)^{3/2}}{(1+a^2v^2)^{5/2}} \frac{1+a^2v^2+3B/2}{1+v^2+B/2} \quad (\text{A22})$$

At  $q^2 \rightarrow 0$  we have  $\Gamma = q^2 D_z$  and thus

$$D_z = A' \pi^{1/2} (1-\alpha)^{1/2} \frac{1+B/2}{1+B} \quad (\text{A23})$$

Finally we have

$$\Gamma = \Gamma_{\text{pre}} + \Delta\Gamma \quad (\text{A24})$$

$$\Gamma_{\text{pre}} = q^2 D_z (1+v^2)^{1/2} \frac{1+v^2/(1+B/2)}{1+v^2/(1+B)}$$

and  $\Delta\Gamma$  as given by eq A21. The coefficients  $C$  in  $\Gamma = q^2 D_z (1 + Cu^2)$  are obtained by power expansion of  $\Gamma$ .

## References and Notes

- (1) P. J. Flory, *J. Am. Chem. Soc.*, **63**, 3083, 3091, 3096 (1941); **69**, 2893 (1947).
- (2) P. J. Flory, "Principles of Polymer Chemistry", Cornell University Press, Ithaca, N.Y., 1953.
- (3) W. H. Stockmayer, *J. Chem. Phys.*, **11**, 45 (1943); **12**, 125 (1944).
- (4) B. H. Zimm and W. H. Stockmayer, *J. Chem. Phys.*, **17**, 1301 (1949).
- (5) L. C. Case, *J. Polym. Sci.*, **26**, 333 (1957); **29**, 455 (1958).
- (6) M. Gordon, *Proc. R. Soc. London, Ser. A*, **272**, 54 (1963).
- (7) G. R. Dobson and M. Gordon, *J. Chem. Phys.*, **41**, 2389 (1964); **43**, 705 (1965).
- (8) D. S. Butler, M. Gordon, and G. N. Malcolm, *Proc. R. Soc. London, Ser. A*, **295** (1966).
- (9) K. Kajiwara, W. Burchard, and M. Gordon, *Br. Polym. J.*, **2**, 110 (1970).
- (10) K. Kajiwara, *J. Chem. Phys.*, **59**, 3623 (1973).
- (11) H. Benoit, *J. Polym. Sci.*, **11**, 507 (1953).
- (12) W. H. Stockmayer and M. Fixman, *Ann. N.Y. Acad. Sci.*, **57**, 334 (1953).
- (13) T. A. Orofino, *Polymer*, **2**, 295, 305 (1961).
- (14) E. F. Casassa, *J. Chem. Phys.*, **37**, 2176 (1962); **41**, 3213 (1964).
- (15) G. C. Berry and T. A. Orofino, *J. Chem. Phys.*, **40**, 1614 (1964).
- (16) C. H. Ruscher and H. Dautzenberg, *Faserforsch. Textiltech.*, **16**, 1 (1965).
- (17) E. F. Casassa and G. C. Berry, *J. Polym. Sci., Part A-2*, **4**, 881 (1966).
- (18) H. Dautzenberg and C. H. Ruscher, *J. Polym. Sci., Part C*, **17**, 2913 (1967).
- (19) W. Burchard, *Macromolecules*, **5**, 604 (1972); **7**, 835, 842 (1974); **10**, 919 (1977).

- (20) I. Franken and W. Burchard, *Macromolecules*, **6**, 848 (1973); *Br. Polym. J.*, **9**, 103 (1977).
- (21) Ch. Wolf and W. Burchard, *Makromol. Chem.*, **177**, 2519 (1976).
- (22) B. Ullisch and W. Burchard, *Makromol. Chem.*, **178**, 1403 (1977).
- (23) M. Müller and W. Burchard, *Makromol. Chem.*, **179**, 1821 (1978).
- (24) B. H. Zimm and R. W. Kilb, *J. Polym. Sci.*, **37**, 19 (1959).
- (25) K. Dušek, M. Ilavsky, and S. Lunak, *J. Polym. Sci., Part C*, **53**, 29 (1975).
- (26) K. Dušek and M. Ilavsky, *J. Polym. Sci., Part C*, **53**, 57 (1975); **57**, 75 (1975).
- (27) B. J. Berne and R. Pecora, "Dynamic Light Scattering", Wiley, New York, 1976.
- (28) B. Chu, "Laser Light Scattering", Academic Press, New York, 1974.
- (29) W. Burchard, *Macromolecules*, **11**, 455 (1978).
- (30) M. Schmidt and W. Burchard, *Macromolecules*, **11**, 460 (1978).
- (31) W. Burchard, M. Schmidt, and W. H. Stockmayer, *Macromolecules*, **13**, 580 (1980).
- (32) K. Kajiwara, *Polymer*, **12**, 57 (1971).
- (33) B. Burchard, K. Kajiwara, M. Gordon, J. Kalal, and J. W. Kennedy, *Macromolecules*, **6**, 642 (1973).
- (34) M. Gordon, K. Kajiwara, C. A. L. Peniche-Covas, and S. B. Ross-Murphy, *Makromol. Chem.*, **176**, 2413 (1975).
- (35) See also M. Hoffmann, H. Krömer, and R. Kuhn, "Polymer-analytik", Vol. 1, Georg Thieme Verlag, Stuttgart, 1977, p 379-83.
- (36) M. Hoffmann and R. Kuhn, *Makromol. Chem.*, **174**, 149 (1973).
- (37) (a) J. E. Hearst and W. H. Stockmayer, *J. Chem. Phys.*, **37**, 1425 (1962); (b) O. B. Ptitsyn and Yu. Ye. Eizner, *Vysokomol. Soedin.*, **3**, 1863 (1961).
- (38) M. Schmidt, D. Nerger, and W. Burchard, *Polymer*, **20**, 582 (1979).
- (39) D. Nerger, Ph.D. Thesis, Freiburg, 1978.
- (40) D. Nerger and W. Burchard, manuscript in preparation.
- (41) W. Burchard, A. Eschwey, I. Franken, and B. Pfannemüller in "Structure of Fibrous Biopolymers", Colston Papers, No. 26, E. D. T. Atkins and A. Keller, Eds. Butterworths, London, 1976, p 365.
- (42) A. Reiner, Diploma Thesis, Freiburg, 1978.
- (43) K. H. Meyer and P. Bernfeld, *Helv. Chim. Acta*, **23**, 865 (1940).
- (44) S. Erlander and D. French, *J. Polym. Sci.*, **20**, 7 (1956).
- (45) G. J. Walker and W. J. Whelan, *Biochem. J.*, **76**, 264 (1960).
- (46) R. S. Whitney and W. Burchard, *Makromol. Chem.*, **181**, 869 (1980).

## Prediction of Glass-Transition Temperatures for Compatible Blends Formed from Homopolymers of Arbitrary Degree of Polymerization. Compositional Variation of Glass-Transition Temperatures. 5

**P. R. Couchman**

*Department of Mechanics and Materials Science, Rutgers University, Piscataway, New Jersey 08854. Received March 6, 1980*

**ABSTRACT:** A model of one-phase mixtures as regular solutions provides the basis of an entropic theory for the prediction of their glass-transition temperatures from pure-component glass-transition temperatures and associated heat-capacity increments. First-order approximations to an initial equation are derived and related to previous equations proposed to describe the composition-dependent glass transition. The phenomenological theory is then applied to the calculation of glass-transition temperatures for one-phase solutions in which the pure components are of arbitrary molecular mass, to give a predictive equation in terms of pure-component chain end and high-polymer glass-transition temperatures and heat-capacity increments. Calculated values of  $T_g$  are found to be in satisfactory accord with experimental glass-transition temperatures for an appropriate binary mixture of polymers. Additionally, the experimental dependence of the Wood parameter on degree of polymerization is accounted for.

### Introduction

The development of a theory for the prediction of composition-dependent glass-transition temperatures for multicomponent mixtures which manifest single glass transitions is of some fundamental interest and, moreover, has practical merit in connection with their processing conditions and in-service properties. In addition, such a theory might serve to clarify the areas of validity of the diverse relations at present used to describe the phenomenon<sup>1-8</sup> in what is for various reasons a somewhat post hoc manner.

As a preliminary step toward the development of a consistent scheme for the calculation of glass-transition temperatures of compatible mixtures from pure-component properties, the first two papers in this series<sup>9,10</sup> were given over in turn to a preliminary discussion of the form such a scheme might take and a phenomenological thermodynamic theory for one-phase solutions of high polymers. The entropic theory<sup>10</sup> was shown to give values of  $T_g$  in close agreement with observed transition temperatures in binary blends of compatible high polymers and

to provide as approximations to a central equation several previous relations for the effect. The third and fourth contributions of the series<sup>11,12</sup> have considered the effect of chain ends on homopolymer glass-transition temperatures as a particular problem in the compositional variation of  $T_g$ , on the premise that polymers of arbitrary molecular mass can be considered single-phase solutions of chain ends and high polymers. Predicted glass-transition temperatures were found to be in satisfactory agreement with dilatometric, calorimetric, and dielectric values of this property<sup>11</sup> and two first-order approximations to a principal equation were shown to give expressions identical in form with previous relations<sup>13,14</sup> for the effect of degree of polymerization on  $T_g$ . Subsequently, the range of comparison between calculated and observed transition temperatures was extended considerably and the relative accuracy of the central relation and the two fundamentally different first-order approximations clarified.<sup>12</sup>

As the theory for composition-dependent glass-transition temperatures has met with a measure of success both for compatible blends of high polymers and for the effect of